



THE UNIVERSITY *of* EDINBURGH

Edinburgh Research Explorer

Effects of nonlinear sound propagation on the characteristic timbres of brass instruments

Citation for published version:

Myers, A, Pyle, RW, Gilbert, J, Campbell, M, Chick, J & Logie, S 2012, 'Effects of nonlinear sound propagation on the characteristic timbres of brass instruments', *The Journal of the Acoustical Society of America*, vol. 131, no. 1, pp. 678-688. <https://doi.org/10.1121/1.3651093>

Digital Object Identifier (DOI):

[10.1121/1.3651093](https://doi.org/10.1121/1.3651093)

Link:

[Link to publication record in Edinburgh Research Explorer](#)

Document Version:

Publisher's PDF, also known as Version of record

Published In:

The Journal of the Acoustical Society of America

Publisher Rights Statement:

Publisher's Version/PDF: subject to Restrictions below, author can archive publisher's version/PDF

Restrictions:

6 months for JASA

General Conditions:

On author's institutional website, governmental websites, as required by authors institution or funder

Authors version only on free E-print servers

Publisher copyright and source must be acknowledged

Publisher's version/PDF may be used on authors own or employers website only

Must link to publisher abstract

Set statements to accompany pre-print and post-print deposit

General rights

Copyright for the publications made accessible via the Edinburgh Research Explorer is retained by the author(s) and / or other copyright owners and it is a condition of accessing these publications that users recognise and abide by the legal requirements associated with these rights.

Take down policy

The University of Edinburgh has made every reasonable effort to ensure that Edinburgh Research Explorer content complies with UK legislation. If you believe that the public display of this file breaches copyright please contact openaccess@ed.ac.uk providing details, and we will remove access to the work immediately and investigate your claim.



Effects of nonlinear sound propagation on the characteristic timbres of brass instruments

Arnold Myers

Reid School of Music, University of Edinburgh, Edinburgh EH8 9AG, United Kingdom

Robert W. Pyle, Jr.

S. E. Shires Co., 11 Holworthy Place, Cambridge, Massachusetts 02138-4509

Joël Gilbert

Laboratoire d'Acoustique de l'Université du Maine, UMR CNRS 6613, 72085 Le Mans Cedex 9, France

D. Murray Campbell

School of Physics and Astronomy, University of Edinburgh, Edinburgh EH9 3JZ, United Kingdom

John P. Chick

School of Engineering, University of Edinburgh, Edinburgh EH9 3JL, United Kingdom

Shona Logie

School of Physics and Astronomy, University of Edinburgh, Edinburgh EH9 3JZ, United Kingdom

(Received 11 December 2010; revised 15 February 2011; accepted 17 February 2011)

The capacity of a brass instrument to generate sounds with strong high-frequency components is dependent on the extent to which its bore profile supports nonlinear sound propagation. At high dynamic levels some instruments are readily sounded in a “cuivré” (brassy) manner: this phenomenon is due to the nonlinear propagation of sound in ducts of the proportions typical of labrosones (lip-reed aerophones). The effect is also evident at lower dynamic levels and contributes to the overall tonal character of the various kinds of brass instrument. This paper defines a brassiness potential parameter derived from the bore geometries of brass instruments. The correlation of the brassiness potential parameter with spectral enrichment as measured by the spectral centroid of the radiated sound is examined in playing tests using musicians, experiments using sine-wave excitation of instruments, and simulations using a computational tool. The complementary effects of absolute bore size on spectral enrichment are investigated using sine-wave excitation of cylindrical tubes and of instruments, establishing the existence of a trade-off between bore size and brassiness potential. The utility of the brassiness potential parameter in characterizing labrosones is established, and the graphical presentation of results in a 2D space defined by bore size and brassiness potential demonstrated.

© 2012 Acoustical Society of America. [DOI: 10.1121/1.3651093]

PACS number(s): 43.75.Fg, 43.25.Ts [TRM]

Pages: 678–688

I. INTRODUCTION: SPECTRAL ENRICHMENT, BRIGHTNESS AND BRASSINESS

The sound of a brass instrument is characterized by a spectrum which is relatively weak in upper harmonics in quiet playing, becoming gradually enriched in upper harmonics during a crescendo. At very high dynamic levels the brightness of the sound increases dramatically; musicians often refer to this timbre as a brassy or “cuivré” effect. These changes in tonal color are among the most basic elements in the performer’s palette of musical expression. One of the principal causes of spectral enrichment in brass instruments is the distributed nonlinear effect due to sound propagation in the bore, which results in a waveform leaving the mouthpiece becoming more and more distorted as it travels along the duct.^{1,2} This effect occurs not only at the very loudest dynamic levels, where in some instruments the nonlinear distortion can result in shock wave formation,³ but is present to a greater or lesser extent at all but the quietest dynamic

levels. The potential for nonlinear wave propagation to occur in a brass instrument at a given dynamic level (described in this paper as the “brassiness potential”) depends on both the bore profile and the absolute bore diameter, and is more significant in instruments with long cylindrical sections of tubing, such as trumpets and trombones, than in instruments which have a higher proportion of steadily expanding tubing, such as flugel-horns and euphoniums. This dependency between bore dimensions and brassiness potential can be exploited as a novel means of distinguishing between different families of brass-wind instruments, and is the subject of this paper.

The approach adopted here is to define a dimensionless parameter, B , which encapsulates the brassiness potential of the instrument based solely on its bore profile normalized to a characteristic dimension D_0 , taken as the minimum diameter at the proximal end.^{4,5} The parameter is independent of other features of the instrument and player coupling which are known to affect the timbre of a played note. Importantly,

the mouthpiece (the dimensions of which have also been shown to have an effect on harmonic content⁶) is ignored. This is justified on the grounds that since mouthpieces are normally interchangeable they are subject to the personal preferences of the player, and in the case of historic instruments, often of uncertain association or absent. It can be seen as an advantage that parameter B represents the contribution of the instrument itself to the *player + mouthpiece + instrument* system.

The brassiness potential parameter B is unaffected by a linear scaling of the radial dimensions of the instrument bore. However, it is commonly accepted by players that radial scale is linked to the rate of spectral enrichment: a narrow bored trombone becomes brassy at a lower dynamic level than a wide bored trombone, for example. Thus a prediction of the spectral enrichment behavior of a brass instrument from bore profile measurements seems likely to require the specification of the two parameters B and D_0 .

The nonlinear coupling between the player and the instrument also has a significant effect on the brightness of a brass instrument sound: even if the lips are opening nearly sinusoidally, a strongly non-sinusoidal flow pattern is generated with rich spectral content except at low dynamic levels.^{7,8} At intermediate dynamic levels the player can have some control over the level of spectral enrichment through manipulation of the embouchure and oral cavity.^{9,10} In testing the utility of the brassiness potential parameter in predicting the degree of spectral enrichment, tests have been carried out with human players,^{4,5} and also using a loudspeaker to generate a sine wave input at the mouthpiece receiver.¹¹ The latter approach has the significant advantage of eliminating both mouthpiece and player variability.

Section II of this paper describes the phenomenon of acoustic wave steepening in flaring instruments and the definition of the brassiness potential parameter B based on the physical dimensions of the instrument. A detailed comparison between B and experimental data taken from a wide range of different brass instruments is presented in Sec. III. These results are also compared with simulations using a computational tool developed specifically to explore nonlinear wave propagation in brass instruments.¹² Section IV attempts to clarify the role of radial bore scale through experiments and simulations on cylindrical tubes. Section V explores the application of the parameters B and D_0 to instrument taxonomy.

II. BRASSINESS POTENTIAL

A. Large-amplitude plane waves

Consider the propagation of a large-amplitude plane wave in an air-filled lossless cylindrical tube.^{13,14} Suppose the initial wave shape is sinusoidal, as shown by the solid curve in Fig. 1. The velocity imparted to the air by the sound wave carries the sound along with it. Thus, dx/dt , the propagation speed at x relative to a fixed observer, is the sum of c , the sound speed relative to the moving air, and u , the particle velocity:

$$\frac{dx}{dt} = c + u. \quad (1)$$

Additionally, the sound pressure alters the local temperature, increasing c where the air is compressed and decreasing it where the air is rarefied. Thus,

$$c = c_0 + \frac{\gamma - 1}{2} u, \quad (2)$$

where γ is the ratio of specific heat at constant pressure to specific heat at constant volume, and c_0 is the small-signal value of the speed of sound. Combining Eqs. (1) and (2) gives

$$\frac{dx}{dt} = c_0 + \frac{\gamma + 1}{2} u. \quad (3)$$

In air, $\gamma = 1.4$, hence the temperature variation increases the effect of convection alone by about 20%.

The speed of the wave as a whole is c_0 , but those parts where the particle velocity u is positive move faster than c_0 and those parts where u is negative move slower than c_0 . This causes the waveform to steepen between a positive peak and the negative peak just ahead of it, as shown by the dashed curve in Fig. 1. Eventually, the rate of change of the waveform becomes infinite and a shock wave is formed.

B. Large amplitude sound in a flaring horn

Next consider waveform distortion in a flaring horn, like a brass instrument. The horn is taken to be of length L and diameter $D(x)$, $0 \leq x \leq L$. The end $x = 0$ is sometimes designated as the “small,” “input,” or “mouthpiece” end of the instrument, and the end at $x = L$ as the “large,” “output,” or “bell” end.

As the sound energy spreads across the increasing cross-section of an outwardly-flaring horn, the particle velocity decreases. If we neglect losses within the horn and assume that the sound energy is spread uniformly across the tube, conservation of energy leads to

$$\frac{u(x)}{u_0} = \frac{D_0}{D(x)}, \quad (4)$$

where $D(x)$ and $u(x)$ are the bore diameter and the particle velocity at position x . D_0 and u_0 are $D(x)$ and $u(x)$ at a reference point. For an entire brass instrument, the reference point is defined to be the point near the input end (within

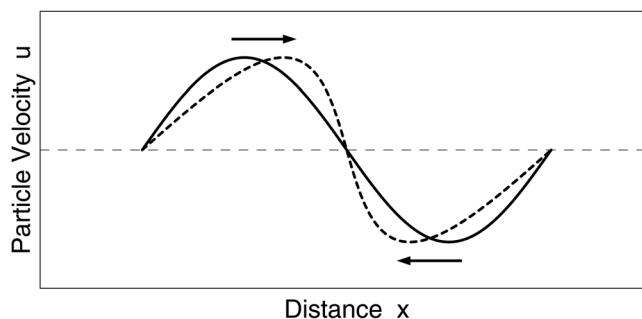


FIG. 1. The solid curve shows one cycle of the initial sine wave, the dashed curve the accumulated distortion at 0.6 times the shock-formation distance. The sound is propagating from left to right. The arrows indicate the direction of particle velocity.

$0 \leq x \leq 0.1L$) where the diameter of the instrument is minimum. This is not *at* the input end, which forms the mouthpiece receiver, but (usually) just beyond the point where the mouthpiece shank ends when the mouthpiece is inserted into the instrument.

Within the flaring horn the sound speed for the various parts of the waveform is changed accordingly. Equation (3) for a plane wave in a cylindrical tube now becomes

$$\frac{dx}{dt} = c_0 + \left(\frac{\gamma + 1}{2}\right) \frac{D_0 u_0}{D(x)}. \quad (5)$$

To achieve the same amount of nonlinear distortion, the sound must travel farther in an outward-flaring horn than in a cylindrical tube, “stretching” the coordinate x .

Figure 2 compares an unstretched cylinder with the stretched x coordinates of a relatively narrow trumpet bell and a more rapidly-expanding flugelhorn bell. Given the same particle velocity injected at the left end, the sound in all three ducts will have achieved the same degree of nonlinear distortion when it arrives at the right end.

The length of a cylindrical tube with the same nonlinear distortion as an entire instrument can be found by integrating Eq. (5) over the whole length of the instrument. For brass instruments that flare outwardly (as virtually all do), it is clear that the length of the cylinder will be less than the length of the instrument.

The *brassiness potential parameter* B is defined as the ratio of the length of that cylinder to L_{ecl} , the equivalent conical length of the instrument. That is,

$$B = \frac{1}{L_{ecl}} \int_0^L \frac{D_0}{D(x)} dx \quad (6)$$

for a bore contour $D(x)$.

The equivalent conical length, L_{ecl} , is the length of a cone, complete to the vertex, whose lowest resonance frequency matches the nominal fundamental frequency of the instrument. Thus L_{ecl} is the same for all instruments pitched in the same key, whereas the physical length L varies slightly among those instruments, depending on their individual bore contours. For a given contour $D(x)$, L_{ecl} is generally about 10% longer than L , the excess being the ‘end correction’ for

that contour. (See Ref. 5 for a more detailed derivation of the definition of B .)

The brassiness potential parameter B is thus a dimensionless number that for normal brass instrument contours always lies between zero and unity. It is higher for “cylindrical” instruments like the trumpet and trombone, and lower for “expanding” instruments like the flugelhorn and euphonium. For the same input signal, larger values of B mean greater nonlinear distortion and therefore a greater tendency for the timbre to acquire a brassy edge at louder dynamics.

C. Calculation of B from bore measurements

For a brass instrument whose sounding length is divided into N sections with arbitrary lengths l_n ($1 \leq n \leq N$), the brassiness potential parameter B as defined in Eq. (6) can be approximated by

$$B \approx \sum_1^N \frac{l_n}{L_{ecl}} \left(\frac{2D_0}{D_{n+1} + D_n} \right), \quad (7)$$

where D_n is the bore diameter at the start of the n th section and D_{N+1} is the diameter at the exit of the final section. It is found that physical measurements of the bore at ten or more points along the length of the tubing give sufficient accuracy. Axial length measurements following the mid-bore line round bends in the tubing can be done with an accuracy of 3% or better. The minimum bore D_0 is usually accessible to direct physical measurement, and can be determined to 0.2 mm (typically within 3% accuracy). Bore measurements along the length of the tube can be estimated to 1% at tuning-slides and other points of separation, and by estimates of bell wall thickness elsewhere (typically to 0.2 mm). The wider tubing of the bell flare makes relatively little contribution to nonlinear propagation effects, and precision is less important here than in the proximal (narrower) part of the bore. The final factor in the calculation of B is the equivalent cone length. For instruments in playing regimes the intended playing pitch is well known and the equivalent cone length can be derived from the nominal pitch and the design pitch standard. In most cases the playing pitch can be estimated by one means or another to within half a semitone, giving an uncertainty in equivalent cone length of less than $\pm 3\%$. Since the brassiness parameter varies widely between families of instruments, its utility is not compromised by errors of the order of 3%.

Measurements of over 1000 instruments of many different kinds, regions of origin and historical periods have been made in performers’ and museum collections, and the value of B computed. Recognized models of instrument show consistency in their B values. Some typical values of B for instruments at 8-ft-9-ft (C-B^b) nominal pitch in the Edinburgh University Collection of Historic Musical Instruments are shown in Table I.

Similar results are found for instruments in other nominal pitches, and where instruments are made in families of different sizes (such as trombones and saxhorns) the values of B for the family members closely match. The distinctions in values of B are less consistent with very small instruments such as trumpets, cornets and flugelhorns in 3(1/2)-ft E^b; it is

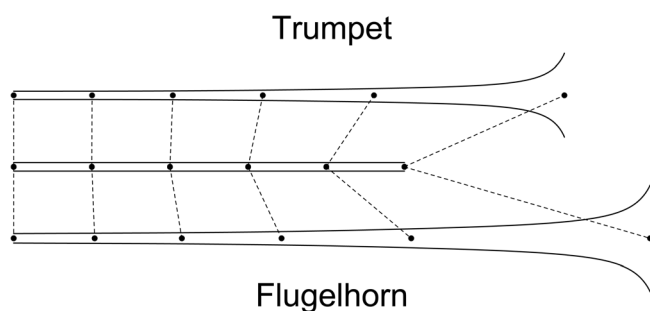


FIG. 2. Three ducts with the same total distortion. At the top is a Vincent Bach model 37 B^b trumpet bell, in the center a cylindrical tube, and at the bottom the final portion of a Salvation Army St. Albans flugelhorn bell. The dashed lines connect intermediate points at which the distortion is the same in all three ducts.

TABLE I. Values of B for typical instruments at 8-ft – 9-ft nominal pitch in the Edinburgh University Collection of Historic Musical Instruments.

Inventory Number	Instrument	Maker	Place	Date	B
(3747)	Tenor trombone, French model	Courtois	Paris	1865	0.81
(3753)	Tenor trombone, German model	Mitsching Alschausky	Germany	c 1935	0.76
(5877)	Bass trombone, modern	Rath	Huddersfield	1999	0.70
(5977)	Tenor trombone, American model	Boosey & Co	London	1926	0.67
(3257)	Bass trumpet	Conn	Elkhart	1929 – 30	0.61
(3887)	Baritone	Boosey & Hawkes	London	1962	0.54
(1804)	Double horn, B \flat side	Alexander	Mainz	c 1950	0.51
(4470)	Saxhorn basse	Ad. Sax	Paris	1864	0.45
(2950)	Euphonium	Besson & Co	London	c 1899	0.40
(2854)	Wagner tuba in B \flat	Alexander	Mainz	c 1930	0.36
(4287)	Ophicleide, keyed for B	Gautrot	Paris	c 1860	0.30

significant that in these cases where the instruments are less strongly characterized the tube length is generally less than the shock length and nonlinear propagation is of less importance.

III. MEASUREMENTS AND SIMULATIONS OF SPECTRAL ENRICHMENT IN BRASS INSTRUMENTS

A. Playing tests on 8-ft and 9-ft instruments with different values of B

The hypothesis that instruments with low values of B develop spectral enrichment more gradually during a crescendo than instruments with high values of B was tested by playing tests carried out on instruments with different bore profiles. Five tenor brasswinds were chosen, with nominally similar pitches, listed in Table II, and shown in Fig. 3.

Three experienced brass players were asked to perform crescendos on each instrument, typically three seconds in duration, from pianissimo to fortissimo. In each case, the note played was the 6th resonant mode, played on the instrument in its natural state (i.e., no valves depressed, first slide position, or all holes closed). The resultant pitch corresponded to musical notation F $_4$ for all instruments, except the ophicleide for which it was E $_4$.

Since B is a characteristic of the instrument only and excludes the mouthpiece, the same mouthpiece was used for all tests: a commercially available Courtois trombone mouthpiece, modified to accommodate a 106B PCB Piezotronics dynamic pressure transducer into the backbore, in a similar manner to that described by Norman *et al.*¹⁰ The radiated sound was also measured using a PCB pressure transducer, located on axis, 0.2m from the plane of the bell exit.

TABLE II. Values of B for the five instruments tested, ranked in descending order of B .

Inventory Number	Instrument, Nominal Pitch	Maker	Place	Date	B
(3205)	Tenor trombone, B \flat	Huschauer	Vienna	1794	0.81
(JG2)	Bass trombone, B \flat + F + G \flat	Courtois	Paris	2000	0.67
(4273)	Saxhorn basse, B \flat	Ad. Sax	Paris	1867	0.51
(3412)	Kaiserbaryton (euphonium), B \flat	Cervený	Königrätz	c 1900	0.37
(3590)	Ophicleide, B \flat , 9 keys	Gautrot	Paris	c 1860	0.31

The signals were split into overlapping segments of 4096 samples each and analyzed with a discrete Fourier transform. The mean value of the instantaneous fundamental frequency and the RMS pressure signals, $p(in)_{rms}$ at input, and $p(out)_{rms}$ at output were estimated for each segment. The normalized spectral centroid (as defined by Beauchamp¹) of the signals measured in the mouthpiece ($SC(in)$) and outside the bell ($SC(out)$) were calculated using Eq. (8):

$$SC = \frac{\sum_n nP_n}{\sum_n P_n}, \quad (8)$$

where P_n is the amplitude of the n th harmonic of the signal.

The calculated values of SC give an indication of the distortion in the signals during the crescendo. As described in Sec. I above, there are two possible sources for the distortion process: (1) the localized nonlinear coupling between the player's lips and the air column, at the entrance of the instrument, and (2) the cumulative nonlinear propagation along the resonator itself. Analysis of $SC(in)$ and $SC(out)$ provides an indication of the relative importance of each of these mechanisms respectively. For tests on the tenor trombone, $SC(in)$ typically increased from 1.2 to 1.6, and $SC(out)$ from 1.5 to 4.0. Although the cumulative nonlinear



FIG. 3. Five brass instruments used in playing tests. From left to right: Kaiserbaryton, ophicleide, bass saxhorn, bass trombone, and tenor trombone.

distortion in the instrument bore clearly dominates at louder dynamics, a significant proportion is due to the localized nonlinear coupling phenomenon. To better understand the contribution of nonlinear propagation in the resonator alone, the ratio $SC(out)/SC(in)$ can be plotted as a function of the normalized input pressure $p(in)_{rms}/P_{atm}$, where P_{atm} is standard atmospheric pressure (1.01325×10^5 Pa); such a plot is shown for one of the players in Fig. 4 (upper graph). Inspection of this figure suggests that the spectral enrichment during the crescendo is highest for the tenor trombone, and least for the ophicleide, as we would expect given the values for B in Table II.

To determine if B is indeed a good indicator of brassiness potential, an empirical function, Eq. (9), with two free parameters A_1 and A_2 , was fitted to the $SC(out)/SC(in)$ data:

$$y = f(x) = A_2[\exp(A_1x) - A_1x]. \quad (9)$$

The best fit curves derived from Eq. (9) are shown in Fig. 4 (lower graph). The collected results from all of the playing tests are shown in Fig. 5, which shows the extracted values of A_1 plotted as a function of B . For each player, A_1 is seen to be a monotonically increasing function of the brassiness potential parameter B , suggesting that B is a valid tool for brass instrument classification.

B. Comparison of B from measurements with spectral centroids in high-frequency amplitude sweeps

Using musicians to sound instruments can lead to results influenced by subjective factors. There are advantages in

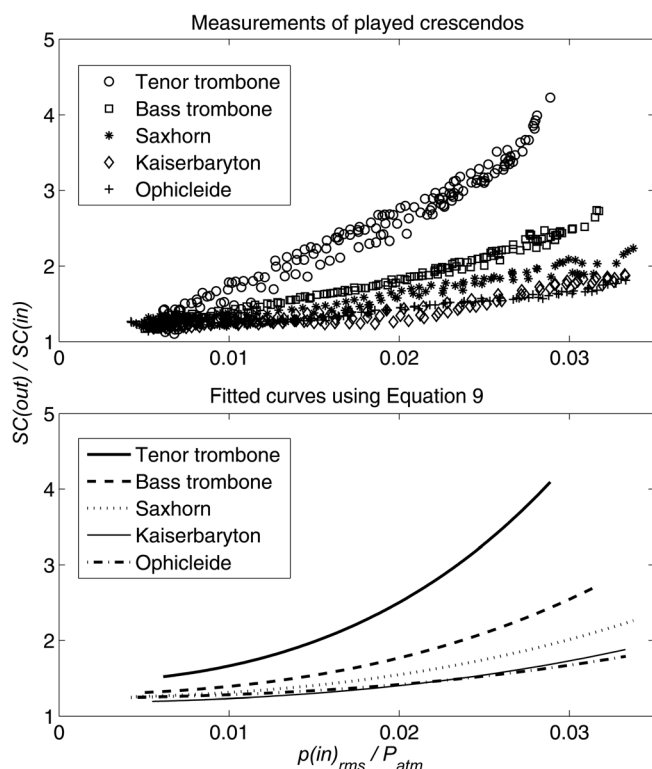


FIG. 4. Experimentally determined ratio $SC(out)/SC(in)$ as a function of normalized input pressure $p(in)_{rms}/P_{atm}$ (upper graph), and the corresponding fit curves using Equation 9 (lower graph). The results are a sample set from one player playing all five instruments (three crescendos per instrument).

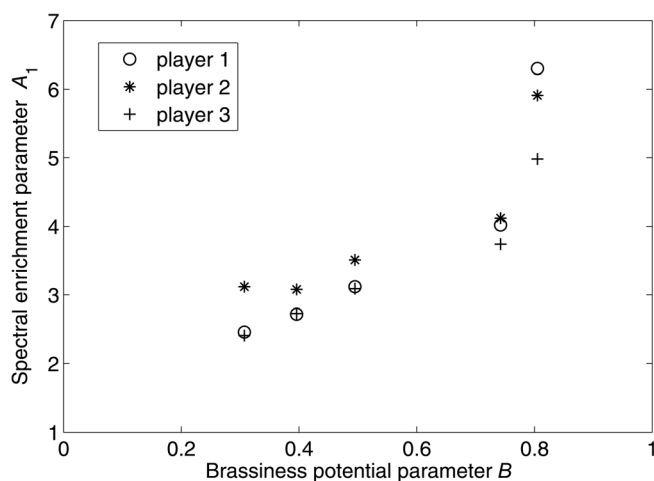


FIG. 5. Values of A_1 as a function of the brassiness potential parameter B for five different instruments tested by three players.

using a loudspeaker which can deliver a sine wave input signal [(spectral centroid $SC(in) = 1$)] at the mouthpiece receiver, resulting in a well-defined curve for the spectral centroid $SC(out)$ of the radiated sound as a function of sound pressure level at input $p(in)_{rms}$ or at output $p(out)_{rms}$. Initial experiments used brass instruments at 8-ft and 9-ft pitch. These had bell flare cutoff frequencies ranging from under 700 Hz (for a euphonium) to around 1100 Hz (for a trombone) and fairly strong low modes of resonance, with relatively little reflection from the bell above 1500 Hz. A pure sine wave excitation was provided by a horn loudspeaker driver coupled to the mouthpiece receiver of the instrument by a short cylindrical insert. A PCB 106B microphone measured the pressure at the coupler entrance, and a Bruel and Kjaer 4192 condenser microphone measured the output at the bell. In each test the sound pressure level at the input was increased from zero to a maximum below the level at which distortion by the loudspeaker was observed in the input signal. The signals from the microphone at the input and the microphone at the bell were simultaneously recorded. The spectral centroid of the signal at the bell gives an indication of the timbre as heard by the audience, in particular the brightening of the timbre as the dynamic is increased, and is calculated in the same way as described in Sec. III A.

The input sine wave frequency was varied, with values selected between 1500 Hz and 3000 Hz. The aim was to find a frequency which was above the bell cut-off frequency and thus minimized internal reflections and standing waves, but not so high that higher order acoustic modes were excited.

Various positions were tried for the position of the microphone at the bell. Two standard positions were used: in the plane of the bell and one meter from the plane of the bell, both on the axis of the bell. The tests were conducted in an anechoic chamber. It was found that the sensitivity of the tests was limited by small frequency-dependent fluctuations (detectable in the plane of the bell even well above cutoff), and by the anisotropy of the far field radiated sound (small directional radiation effects at one meter from the plane of the bell).

These limitations on the sensitivity of the tests meant that small changes in instrument settings (such as a semitone difference in valve or trombone slide positions) produced changes in the spectral centroid which could not reliably be detected, but larger changes in instrument settings (such as five semitones difference in valve or trombone slide positions) produced distinct changes in the spectral centroid. These could then be compared with values of the brassiness potential parameter B derived from bore geometries and the spectral enrichment predicted by simulation.

Figure 6 shows the spectral centroid of the radiated sound $SC(out)$ at the plane of the bell with a sine wave input of frequency 2500 Hz for four instruments at 8-ft or 9-ft pitch, plotted against the normalized sound pressure $p(in)_{rms}/P_{atm}$. Measurement in the plane of the bell was chosen in this case to facilitate comparison with the simulation results described in Sec. III C. It is evident from Fig. 6 that the rate of spectral enrichment is much higher for the trombone ($B = 0.70$) than for the ophicleide ($B = 0.30$); this is consistent with the behavior observed in the results from human players shown in Fig. 4. However, although the cornophone and Kaiserbaryton have significantly different values of B (0.43 and 0.37, respectively), they are indistinguishable in the spectral enrichment measured using sine wave excitation.

Experimental tests on a large number of brass instruments have shown the same behavior: differences in the brassiness potential parameter B generally correlate well with differences in measured rates of spectral enrichment, but from time to time pairs of instruments are found in which the correlation is either absent or reversed. A possible explanation for this phenomenon in terms of the absolute radial scale parameter D_0 is presented in Sec. IV.

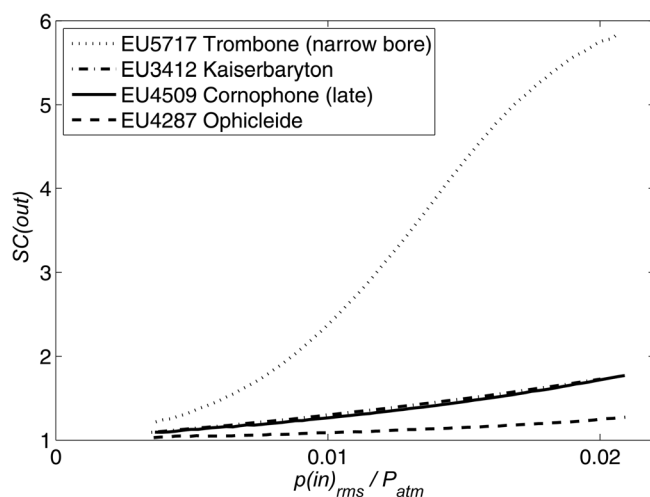


FIG. 6. Plots of spectral enrichment measured in amplitude sweeps of sine wave excitation at 2500 Hz of four instruments in Edinburgh University Collection of Historic Musical Instruments. The spectral centroid at the plane of the bell is plotted against normalized RMS sound pressure at the mouthpipe. The respective values of B computed from physical measurements are: (5717) tenor trombone in 9-ft B \flat (Hawkes & Son, London, c 1928) 0.70; (4509) cornophone tenor in 8-ft C (Besson, Paris, 1905–10) 0.43; (3412) Kaiserbaryton in 9-ft B \flat (Cervený, Königgrätz, c 1900) 0.37; (4287) ophicleide, keyed for B (Gautrot, Paris, c 1860) 0.30.

C. Comparison of B from measurements with spectral enrichment curves from simulations

In order to shed further light on the experimentally observed behavior described in Secs. III A and III B, the spectral enrichment for many of the instruments studied was simulated using the computational tool described by Gilbert.¹² This calculates the pressure and velocity acoustic fields everywhere inside the bore using the weakly nonlinear approximation, taking as inputs the pressure signal $p(in)$ at the entrance to the instrument, a radiated impedance boundary condition at the output end, and the bore geometry of the instrument. The simple waves propagating in each direction, assumed not to interact in the body of the fluid, are solutions of the Generalized Burgers' equations.

The simulated spectral enrichment behavior for the four instruments discussed in Sec. III B is illustrated in Fig. 7. For each instrument, the terminating impedance was approximated by the radiation impedance for an unflanged cylinder with the same diameter as the bell. Comparison of Figs. 6 and 7 shows that there is good agreement between experiment and simulation in the case of the narrow bore trombone. For the other three instruments, the rate of spectral enrichment predicted by simulation is consistent with the ranking by brassiness potential parameter, but is greater than that measured experimentally. One possible reason for this discrepancy is that the plane wave approximation used in the simulation tool is likely to be less satisfactory in more widely flaring instruments; another is that the more complex internal geometry of the keyed and valved instruments could give rise to additional localized nonlinear losses and leaks.

IV. EFFECT OF ABSOLUTE RADIAL SCALE ON SPECTRAL ENRICHMENT

A. Transfer functions in the linear regime

The brassiness potential parameter B for a particular instrument is based on a calculation of the length of cylindrical tubing which would generate the same degree of wave

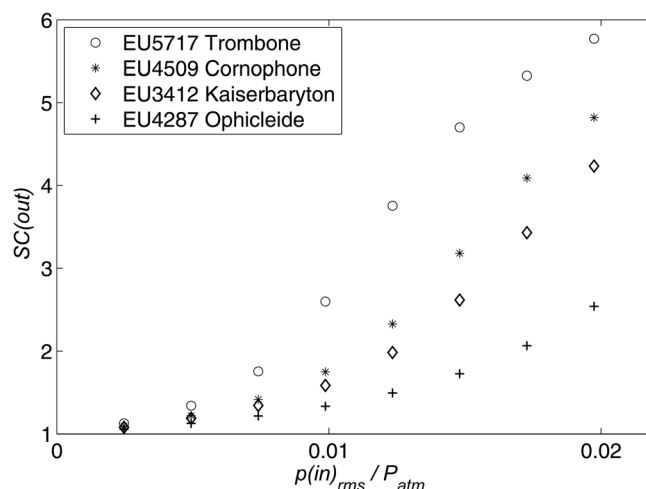


FIG. 7. Plots of simulated spectral enrichment of the same instruments as in Fig. 6. The spectral centroid at the plane of the bell is plotted against normalized RMS sound pressure at the mouthpipe for a sine wave input with frequency 2500 Hz.

distortion for a given pressure input. In this calculation viscothermal wall losses are assumed to be negligible. The distance X_s required for the generation of a shock wave in a cylindrical tube is given in this lossless approximation by³

$$X_s \approx \frac{2\gamma P_{atm} c}{(\gamma + 1)(\delta p(in)/\delta t)_{\max}}. \quad (10)$$

where $p(in)$ is the input pressure, P_{atm} atmospheric pressure, c the speed of sound in air and γ the ratio of specific heats for air. It can be seen from Eq. (10) that X_s is not dependent on the internal diameter of the tube D ; tubes of different diameter but the same length should therefore have the same rate of nonlinear distortion for the same input pressure waveform.

It was pointed out in Sec. I that musicians expect a narrow bored brass instrument to develop a brassy timbre at a lower dynamic level than a wide bored instrument of similar relative bore profile (and therefore B value). One factor justifying this expectation is that the musician's judgement of dynamic level relates to the pressure in the radiated sound field rather than the pressure inside the instrument. In the linear acoustic limit a sine wave input pressure $p(in)$ generates a radiated sine wave output pressure $p(out) = Tp(in)$, where T is the transfer function between the instrument input and the measurement point in the radiation field. For frequencies low enough that the wavelength is much greater than the bell diameter, the radiation can be approximately treated as that of a monopole source centered on axis in the bell exit plane:

$$\begin{aligned} p(out) &\approx \frac{j\rho_0\omega Q}{4\pi d} \exp(j\omega t - kd) \\ &\approx \frac{\rho_0\omega S u(bell)}{4\pi d} \exp(j(\pi/2 - kd)), \end{aligned} \quad (11)$$

where d is the distance from the monopole source to the measurement point, S is the area of the bell opening, $u(bell)$ is the acoustic particle velocity at the bell exit plane and Q the monopole source strength. Then

$$T = \frac{p(out)}{p(in)} = \frac{\rho_0\omega S}{4\pi d} \exp(j(\pi/2 - kd)) \frac{u(bell)}{p(in)}. \quad (12)$$

Neglecting the effect of viscothermal wall losses in the tube, the ratio $u(bell)/p(in)$ will be unaffected by a uniform radial scaling of the bore by a factor σ . Since T is proportional to the bell area S it will increase by a factor σ^2 . The minimum diameter D_0 will increase by a factor σ , so that this lossless approximation predicts that $T \propto D_0^2$.

For most of the brass instruments in the present study, the wavelength is equal to the bell diameter at a frequency of approximately 1.5 kHz, corresponding to the 25th harmonic of the nominal pitch for an 8-ft B^b instrument. The monopole approximation will not therefore describe adequately the radiation of high frequency components, but the foregoing discussion illustrates the expected dependence of the transfer function on radial bore scale in the low frequency limit.

Wall losses reduce $u(bell)/p(in)$ by an amount which increases as the internal diameter is reduced. This effect

further increases the dependence of T on D_0 . For a cylindrical tube of length L with input at $x = 0$ the effect of losses on the transfer function can be taken into account by introducing the complex wave vector $k' = \omega/v - j\alpha$, where v is the propagation velocity inside the tube and α is the viscothermal attenuation coefficient.¹⁵ Treating the internal sound field as the sum of a forward propagating wave $p_+ = A \exp(j(\omega t - k'x))$ and a backward propagating wave $p_- = B \exp(j(\omega t + k'x))$, the input pressure and output particle velocity can be expressed as

$$p(in) = (A + B) \exp(j\omega t), \quad (13)$$

$$\begin{aligned} u(out) &= (\rho_0 c)^{-1} [A \exp(-jk'L) \\ &\quad - B \exp(jk'L)] \exp(j\omega t). \end{aligned} \quad (14)$$

Equation (12) can then be expressed in the form

$$T = \frac{kS \exp(j(\pi/2 - kd))}{2\pi d [(Z_L/Z_0 + 1) \exp(jk'L) + (Z_L/Z_0 - 1) \exp(-jk'L)]}, \quad (15)$$

where Z_L is the radiation impedance and $Z_0 = \rho_0 c/S$ the characteristic impedance of the tube.

As an illustration of the effect of losses on the transfer function, the value of T for a cylindrical tube of internal diameter 13.5 mm and length 2.36 m at a frequency $f = 3000$ Hz and a distance $d = 0.5$ m is 1.30×10^{-3} when the calculation ignores wall losses; the inclusion of losses reduces T by 18% to 1.07×10^{-3} . This diameter of tubing is typical of that used in the slide section of a tenor trombone. For a tube of the same length but with diameter reduced to 6.4 mm, the corresponding figures are 2.4×10^{-4} (ignoring losses) and 1.56×10^{-4} (including losses); in this case the wall losses have reduced the transfer function by 35%.

B. Transfer functions in the nonlinear regime

The dependence of the linear transfer function on the bore diameter implies that a musician needs to generate a higher amplitude input pressure $p(in)$ in a narrow bored instrument than in a wide bored instrument in order to radiate the same sound intensity. Equation (10) then implies that the rate of nonlinear distortion will be larger in the narrow bored instrument.

It is difficult to quantify this effect, since when the output waveform is significantly distorted the concept of a linear transfer function is no longer applicable. An input sine wave results in an output harmonic spectrum whose spectral centroid increases with the degree of nonlinear distortion, up to the point at which a shock wave is formed. The higher frequency components are more effectively radiated because of the frequency dependence of the radiation impedance, so that the total radiated sound power for a given input pressure also increases with the degree of nonlinear distortion. This increase in radiated sound power is partially counteracted by the increased wall losses due to the frequency dependence of the attenuation coefficient.

The perceived dynamic level of the radiated sound will depend on many factors, including the frequency response of

the human ear, the influence of mutual masking of frequency components, and the musical context in which the judgement is made. In the present study a simplified effective transfer function, applicable to the nonlinear distortion case, has been defined as

$$T_{eff} = p(out)_{rms}/p(in)_{rms}. \quad (16)$$

To examine the dependence of the effective transfer function and the degree of spectral enrichment on the radial scale parameter D_0 , experiments and simulations were carried out using high frequency sine wave excitation in cylindrical tubes.

C. Measurements of nonlinear distortion in cylindrical tubes

Using the experimental arrangement described in Sec. III B, three cylindrical tubes were studied. Each was 2.36 m long, and their internal diameters were 13.5 mm, 9.4 mm and 6.4 mm respectively. The 13.5 mm internal diameter tube was copper, with external diameter 15 mm; the other two tubes were stainless steel, with external diameter 13 mm. The input sine wave had a constant frequency of 3000 Hz, with a linear amplitude sweep from 0 Pa to approximately 3 kPa in 2 s. The microphone at the output was positioned on axis at a distance $d = 0.5$ m in each case.

The upper graph in Fig. 8 shows the measured evolution of the effective transfer function during the crescendo for each of the tubes. The upper graph in Fig. 9 illustrates the

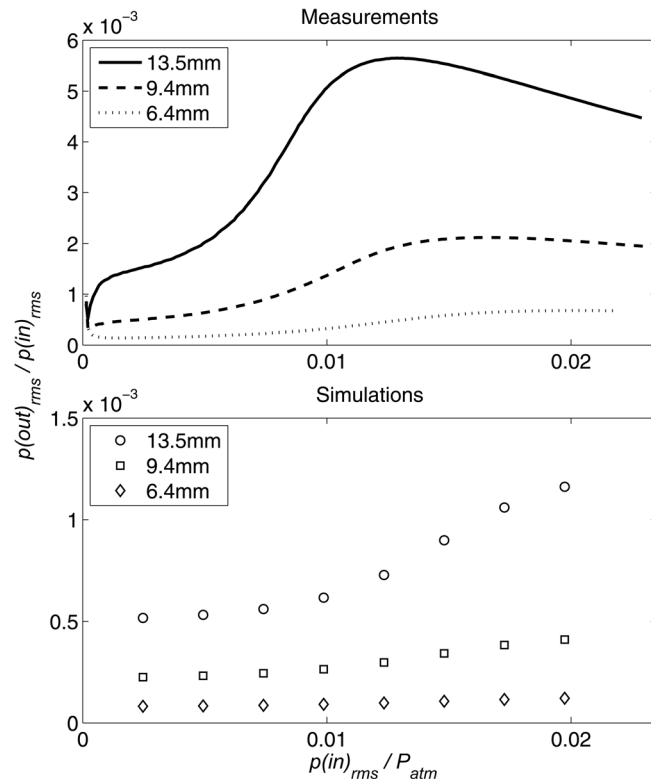


FIG. 8. Effective transfer functions for three cylindrical tubes, each of length 2.36 m, with internal diameters 13.5 mm, 9.4 mm and 6.4 mm respectively. The excitation frequency was $f = 3000$ Hz, and the output pressure was measured at a distance $d = 0.5$ m from the cylinder end, on axis. Upper graph: measurements; lower graph: simulations.

rise in the spectral centroid of the radiated sound during the crescendo for each tube. The values of T_{eff} for $p(in)_{rms}/P_{atm} = 0.002$ are similar to those calculated using Eq. (15), suggesting that the system behavior at this input pressure is close to linear; however, the fact that the spectral centroid is greater than one for each tube shows that a small degree of distortion is already evident. The rapid rise in the spectral centroid with increasing $p(in)$, which is a measure of the spectral enrichment arising from nonlinear distortion, is accompanied as expected by a dramatic increase in the effective transfer function. When the transfer function is calculated using only the first harmonic of $p(out)$, experimental and simulated results both show a slow decrease with increasing $p(in)$, confirming that energy is being transferred from the first harmonic into higher harmonic components.

Equation (10), based on the lossless approximation, predicts that a shock wave will form within each of the cylindrical tubes at an input pressure $p(in)_{rms}$ of approximately $0.006P_{atm}$. The rate of increase in the spectral centroid is a maximum at around this value for the 13.5 mm diameter tube, for which wall losses are least significant. The rate of increase in the spectral centroid with pressure diminishes as the tube radius is reduced, showing the increasing importance of wall losses in reducing the degree of spectral enrichment to be expected at a given input pressure.

D. Simulations of nonlinear distortion in cylinders

The lower graphs in Figs. 8 and 9 show the results of simulations of nonlinear propagation in the three cylinders

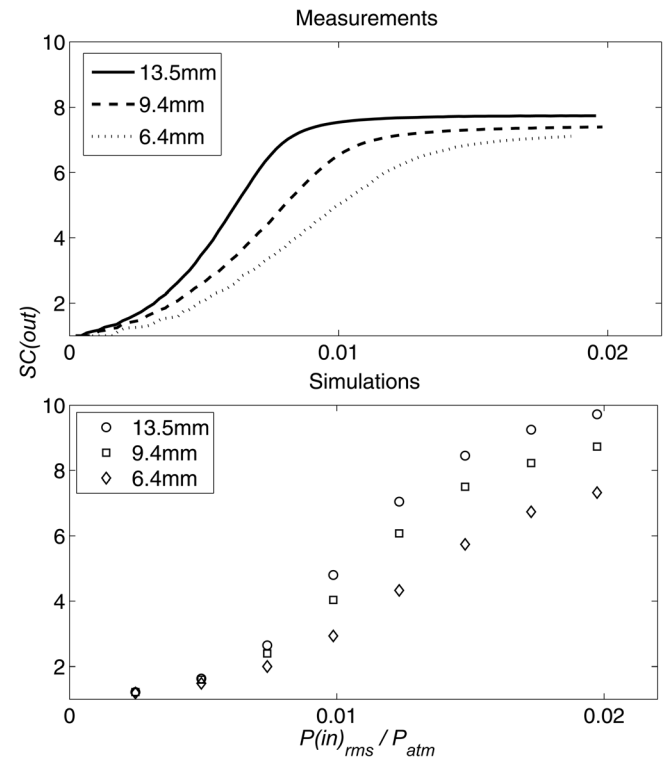


FIG. 9. Spectral centroid of sound radiated by three cylindrical tubes, each of length 2.36 m, with diameters 13.5 mm, 9.4 mm and 6.4 mm, respectively. The excitation frequency was $f = 3000$ Hz, and the output pressure was measured at a distance $d = 0.5$ m from the cylinder end, on axis. Upper graph: measurements; lower graph: simulations.

described in Sec. IV C, using the computational method described in Sec. III C. To provide a direct comparison with the measurements, the simulated output pressure was calculated for a point on the cylinder axis at a distance of 0.5 m from the exit, assuming monopole radiation.

The simulated effective transfer functions shown in Fig. 8 (lower graph) are smaller than the measured values by a factor of between two and three at low input pressures, and grow more slowly as the input pressure increases. The effect of the bore diameter on the transfer function is however apparent. The simulations of spectral centroid evolution during a crescendo, shown in Fig. 9 (lower graph), again confirm the expected trends, although predicting a slower spectral enrichment than was observed experimentally.

The reasons for the quantitative differences between the experimental measurements and simulation results are not clear, although a significant factor is likely to be the failure of the monopole radiation approximation at the higher frequencies which are introduced by nonlinear distortion. For the 13.5 mm diameter cylinder with a 3 kHz input, the ratio of wavelength to diameter is 8.5 for the fundamental component; it reduces to 0.6 for the 15th harmonic, the highest component analyzed in the production of Fig. 9. Thus although the radiation of the fundamental will be approximately isotropic, the energy transferred to the higher harmonics will be preferentially radiated along the cylinder axis, increasing the measured spectral centroid. The concentration of the radiated sound intensity in the central lobe of the directivity pattern could also lead to significant additional nonlinear steepening of the wavefront beyond the cylinder exit.

Localized nonlinear effects due to flow separation and vortex shedding at the cylinder exit, which are not taken into account in the simulation, could also significantly affect the radiated sound field. Vortex shedding will introduce additional losses preferentially absorbing low frequency components in the acoustic field, thus increasing the measured spectral centroid. These nonlinear losses will have been accentuated by the fact that the internal edges of the cylinder ends were not rounded, but left as sharp right angles.¹⁶

E. Simulating the effect of radial scale in musical instruments

The experiments and simulations using cylindrical tubes have confirmed that both the bore diameter D_0 and the brassiness potential parameter B are important in determining the spectral enrichment due to nonlinear sound propagation.

To explore the effect of bore diameter on spectral enrichment in realistic musical instruments, playing tests and laboratory experiments using sine wave excitation have been undertaken.¹¹ A major difficulty in this approach is that of finding instruments differing in radial scale but having otherwise identical bore profiles. Such instruments can however be easily constructed in the virtual domain, and the simulation method then allows the effects of radial scale changes to be explored. Figure 10 shows simulations of

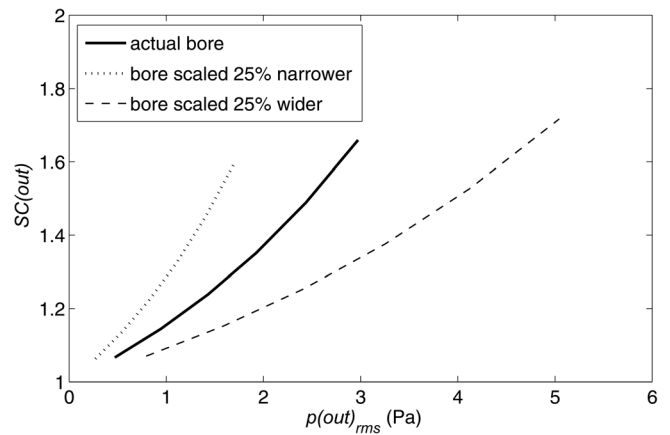


FIG. 10. Plots of simulated spectral enrichment of (4509) Cornophone tenor in 8-ft C (Besson, Paris, 1905–10) calculated for the actual bore (solid line), and also for the entire bore scaled down in diameter by 25% (dotted line) and up in diameter by 25% (dashed line). The excitation frequency was 2500 Hz, and the output pressure was calculated 1 m from the bell plane, on axis.

spectral centroids measured in the far field (1 m from bell plane, on axis of bell) against amplitude at the far field for instruments scaled down and scaled up while retaining the same relative bore profile and therefore the same value of B . The effect of bore size on spectral enrichment for a given dynamic output is clearly shown.

V. TAXONOMY OF LABROSONES

A. The $B - D_0$ scatter plot as a taxonomic tool

There is evidently a strong effect of absolute bore size on spectral enrichment in the far field for a given dynamic output (measured by rms pressure) of instruments with identical values of B . It is not possible at this stage to quantify the trade-off between B and absolute bore size and this may prove to be complex if it is frequency dependent. The theoretical, experimental and computational studies described in Sec. IV provide a physical justification for the use as a taxonomic tool of scatter plots with B on one axis and D_0 on the other. This clearly separates recognized models of

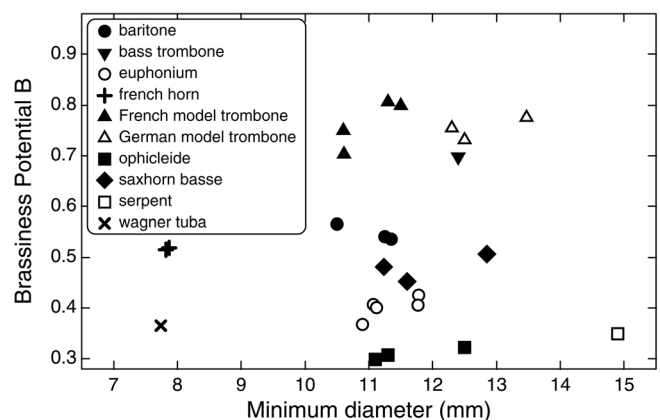


FIG. 11. Scatter plot of the brassiness potential parameter B computed from physical measurements, plotted against the minimum diameter D_0 , for 26 instruments of conventional design in Edinburgh University Collection of Historic Musical Instruments.

instrument such as euphoniums and Wagner tubas which, as seen in Table I, have similar values of B but different values of D_0 . One such scatter plot is given in Fig. 11.

Once the areas which are occupied by instruments of recognized design within such a scatter plot are established, instruments of problematic identity can be measured and B computed. Their position in relation to other instruments should then give an indication of their timbral properties.

B. Effects of use of valves and slides

So far, instruments have been considered to have a single bore profile, that of the instruments with their shortest tube length. For most valved instruments the shortest tube length is obtained with no valves operated; for slide trombones it is obtained with the slide in closed position. The simple assumption has been made that the use of slides, valves and other devices which change the sounding length of an instrument can be ignored, and that chromatic instruments can be treated as equivalent to natural instruments. Nevertheless, in normal playing of a chromatic brass instrument the sounding length differs from the length associated with the nominal pitch of the instrument for most of the notes sounded. A chromatic brass instrument places in effect a group of tubes of differing lengths in the hands of a player. There is a range of B values corresponding to the different valve or slide positions (for a three-valve instrument or a normal trombone slide there will be seven values of B associated with the seven positions). Since D_0 is unaffected by the operation of valves and slides, each point on the scatter plot in Fig. 11 will be at the lower end of a series of typically seven points in a vertical line representing seven valve or slide positions.

To explore the significance of this effect, a series of measurements of spectral enrichment was carried out for a number of instruments with valves or slides set to give the shortest tube length and to give longer tube lengths. Values of the brassiness potential parameter were calculated for the corresponding physically measured bore geometries. In addi-

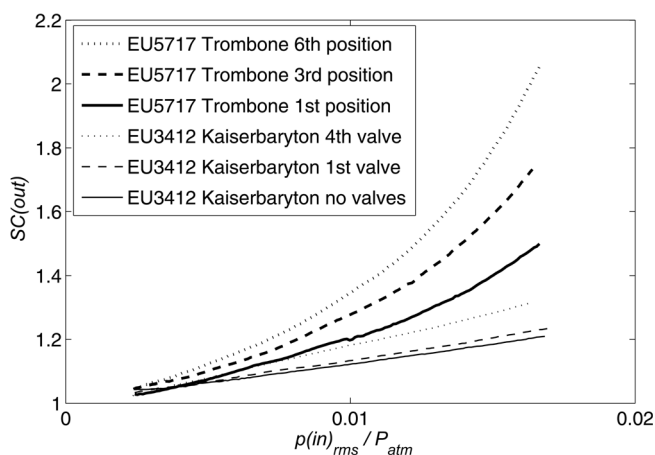


FIG. 12. Increase of radiated spectral centroid with input sound pressure level for a narrow-bore trombone by Hawkes (EUCHMI 5717) in 6th, 3rd, and 1st positions ($B = 0.72, 0.71$ and 0.70 , respectively), and for a Kaiserbaryton (wide-bore euphonium) by Cervený (EUCHMI 3412) with 4th valve, 1st valve, and no valves ($B = 0.42, 0.40$ and 0.36 , respectively).

tion, spectral enrichment was theoretically simulated for the various tube lengths available with a single instrument.¹⁷ Figure 12 shows the spectral centroid of the sound radiated in response to excitation by a sine wave with frequency 1500 Hz, plotted as a function of input sound pressure for an instrument with a high value of B (highest three curves), and for an instrument with low value of B (lowest three curves).

Although the spread in values of B is greater for the wide-bore euphonium with different fingerings, the effect of changing fingerings on the spectral centroid appears to be less than for the narrow-bore trombone with different slide positions where the spread in values of B is less. On an instrument with low brassiness potential, operating the valves clearly has a big effect on the value of B , yet a euphonium or tuba gives the listener the impression of a consistent sound quality in passages that move across differing tube lengths. This effect is probably due to the low incidence of nonlinear propagation resulting from the wide bore and the relatively small pressure amplitudes required to produce the dynamic levels commonly used in tuba music.

To characterize a chromatic instrument it is convenient to assign a single value of the brassiness potential parameter to the instrument as a whole: this has to be a single tube, which could be either the shortest, or one representing an average for the instrument. Since an average in most cases is only slightly longer than the shortest, and is arbitrarily defined, use of the bore profile of the shortest seems the most practical decision.

VI. CONCLUSIONS AND FURTHER WORK

Theoretical considerations, laboratory measurements, and simulations show correlated rankings between spectral enrichment as measured using the spectral centroid and the brassiness potential parameter B derived from the bore geometry of brass instruments. B as defined in this paper has been computed for over 1000 instruments with consistent results. It has also been shown that the absolute radial scale of an instrument, measured by the minimum diameter D_0 at the input end, affects the rate of spectral enrichment for instruments with identical B values through two competing mechanisms: the increase in effective transfer function with D_0 allows the musician to generate a given dynamic level with a lower input pressure and therefore less distortion, while the reduced effect of wall losses in wider tubes increases the efficiency with which the higher frequencies are transmitted.

Scatter plots such as Fig. 11, presenting a population of instruments in a 2D space defined by bore size and brassiness potential, can successfully divide instruments with different basic tube lengths into recognized families, although the very shortest instruments do not have such well-defined areas in this space. Brassiness potential is an effective tool which not only categorizes recognized models of instruments but also allows the placement of historical and lesser-known models within a common framework according to parameters which reflect their acoustical behavior. This is particularly valuable in the case of historic instruments which are not in playable condition.

Further work is needed to establish the level of resolution of the computed values of B : the smallest differences in B which are consistently measurable or detectable by musicians. Laboratory measurements of spectral enrichment have proved to be limited in resolution by the small frequency-related effects and the existence of anisotropy in the radiated sound: greater resolution should be obtainable using a microphone array rather than the single microphone used in the work described here. The trade-off between bore size and brassiness potential suggests that it might be possible to define contours of equal levels of spectral enrichment for similar far field loudness on the plots in B and D_0 , though it cannot be assumed that such contours would be independent of dynamic level and frequency.

ACKNOWLEDGMENTS

The authors gratefully acknowledge the participation in experimental studies of nonlinear propagation in brass instruments by current and former students at the University of Edinburgh, including Samuel Stevenson, Rob Macdonald, Michael Newton, Seona Bromage, Lisa Norman, Pierre Aumond, Nicolas Barascud and Lucile Rutkowski. Adam Apostoli developed the Labview programs used in the sine wave excitation studies, and valuable technical assistance was provided by Les Russell at Edinburgh and Emmanuel Brasseur at Le Mans. The authors are also indebted to the anonymous referees for several very helpful suggestions. Part of this research was supported by an EPSRC Doctoral Training Grant.

¹J. W. Beauchamp, "Synthesis by spectral amplitude and brightness matching of analyzed musical instrument tones," *J. Audio Eng. Soc.* **30**, 396–406 (1982).

²J. Beauchamp, "Analysis of simultaneous mouthpiece and output waveforms," Audio Engineering Society preprint Paper No. 1626 (1980).

³A. Hirschberg, J. Gilbert, R. Msallam, and A. Wijnands, "Shock waves in trombones," *J. Acoust. Soc. Am.* **99**(3), 1754–1758 (1996).

⁴A. Myers, J. Gilbert, R. Pyle, and D. Campbell, "Non-linear propagation characteristics in the evolution of brass musical instrument design," in *Proceedings, 19th International Congress on Acoustics*, Madrid (September 2–7, 2007), pp. 1–6.

⁵J. Gilbert, D. Campbell, A. Myers, and R. Pyle, "Difference between brass instruments arising from variations in brassiness due to nonlinear propagation," in *Proceedings of the International Symposium on Musical Acoustics (ISMA)*, Barcelona (September 9–12, 2007), pp. 1–8.

⁶E. Poirson, J.-F. Petiot, and J. Gilbert, "Study of the brightness of trumpet tones," *J. Acoust. Soc. Am.* **118**, 2656–2666 (2005).

⁷J. Backus and T. Hundley, "Harmonic generation in the trumpet," *J. Acoust. Soc. Am.* **45**, 509–519 (1971).

⁸S. Elliot and J. Bowsher, "Regeneration in brass and woodwind instruments," *J. Sound Vib.* **83**, 181–217 (1982).

⁹L. Norman, J. Chick, D. Campbell, and A. Myers, "Embouchure control of brassiness at constant pitch and dynamic level in orchestral horn playing," in *Proceedings of the NAG-DAGA International Conference on Acoustics*, Rotterdam (March 23–26, 2009), pp. 862–865.

¹⁰L. Norman, J. Chick, D. Campbell, A. Myers, and J. Gilbert, "Player control of 'brassiness' at intermediate dynamic levels in brass instruments" *Acust. Acta Acust.* **96**, 614–621 (2010).

¹¹A. Myers, R. Pyle, J. Gilbert, and D. Campbell, "The influence of bore size on brassiness potential," in *Proceedings of the 2nd Vienna Talk on Music Acoustics*, University of Music and Performing Arts, Vienna (September 19–21, 2010), pp. 102–105.

¹²J. Gilbert, L. Menguy, and D. Campbell, "A simulation tool for brassiness studies," *J. Acoust. Soc. Am.* **123**, 1854–1857 (2008).

¹³D. T. Blackstock and M. J. Crocker, "Nonlinear acoustics and cavitation," in *Encyclopedia of Acoustics*, edited by M. J. Crocker (Wiley, New York, 1997), Chap. 17, pp. 193–195.

¹⁴M. Hamilton and D. Blackstock, eds., *Nonlinear Acoustics* (Academic Press, New York, 1998), pp. 57–59.

¹⁵N. H. Fletcher and T. D. Rossing, *The Physics of Musical Instruments*, 2nd ed. (Springer, New York, 1998), pp. 193–205.

¹⁶J. M. Buick, M. Atig, D. J. Skulina, D. M. Campbell, J. P. Dalmont, and J. Gilbert, "Investigation of nonlinear acoustic losses at the open end of a tube," *J. Acoust. Soc. Am.* **129**, 1261–1272 (2011)

¹⁷A. Myers, J. Gilbert, R. Pyle, and D. Campbell, "The brassiness potential of chromatic instruments," in *Proceedings of Congres Francais d'Acoustique*, Lyon, Lyon (April 12–16, 2010), pp. 1–4.